# Master's Project (ongoing)

## Dark state pair-production in underground accelerators and their detection

Supervised by Josef Pradler

Fahrecker Maximilian

Seminar on Particle Physics

Faculty of Physics, University of Vienna

28th of May 2024

# OUTLINE

We want to theoretically explore the possibility of new light particles with a novel experimental set-up.

Problem: light dark matter in our solar system is difficult to detect due to its small velocity

Idea: produce new particles at relativistic speeds, then detecting them using semiconductors at the underground laboratory in Modane, France

# Dark Matter

- Dark matter (DM):
  - Introduced by Zwicky to explain missing mass in galaxy clusters
  - Subsequently explains for galactic rotation curve and CMB
- DM is now part of standard cosmology
- Numerous models for particle DM, examples include
  - WIMPs: Weakly Interacting Massive Particles
  - Axions: very light particles, can solve strong CP Problem
- DM experiments usually constrain parameter space

# Dark Matter Search

- GeV mass DM is well explored
- Sub-GeV and sub-MeV DM still relatively unprobed
- Low mass DM becoming more accessible

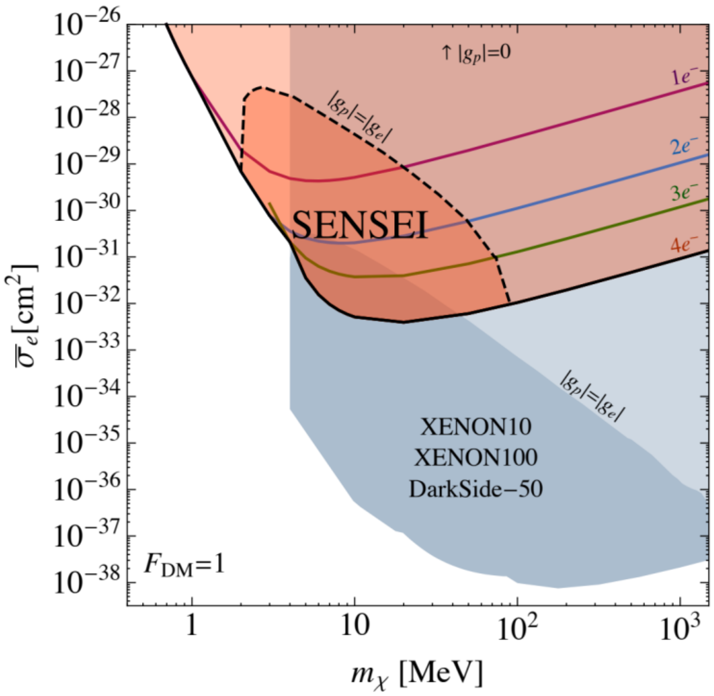


From: [Crisler and SENSEI collab., 2018, arXiv:1804.00088]

From: [Billard et al., 2021, arXiv:2104.07634]

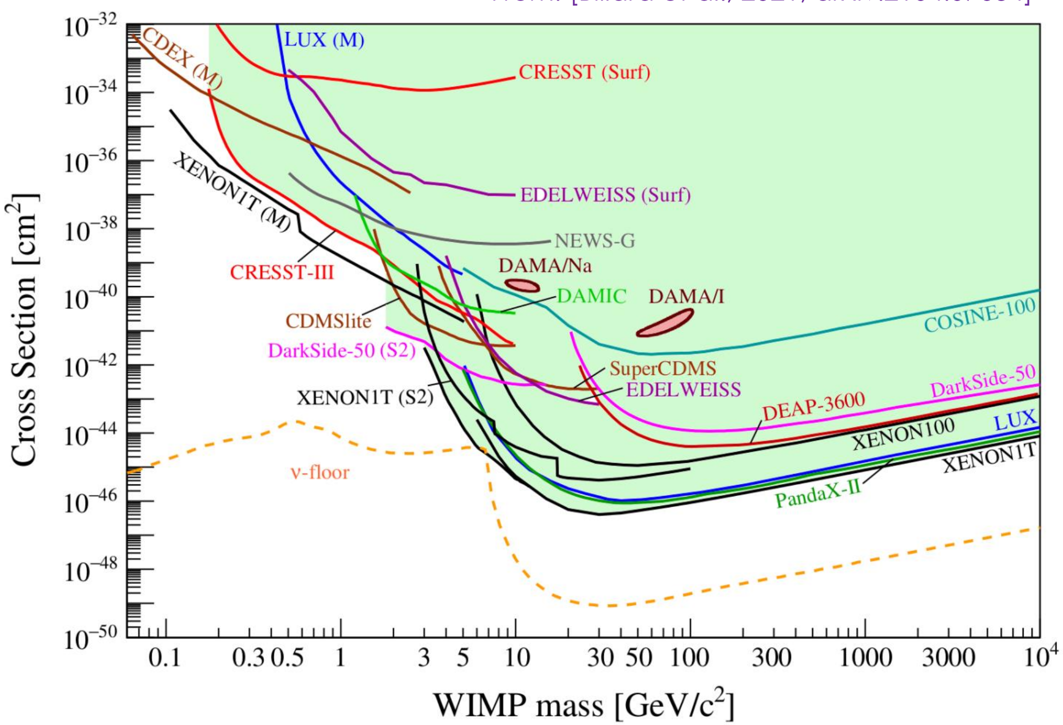

# DM DIRECT DETECTION

- Scattering on nuclei and electrons of bulk
- Very heavy DM scattering dominated by DM-Nucleus interaction → scales with detector mass
  - Examples: XENONnT, EDELWEISS, CRESST
- Recently, semiconductor detectors like CCDs
  - Examples: SENSEI, DAMIC
- We investigate DM-electron scattering in a novel CCD experiment called DAMIC-M

# Reminder: Charge-Coupled Device

CCDs use doped semiconductors, mostly silicon, to collect charge carriers created by the photoelectric effect or other scattering events.

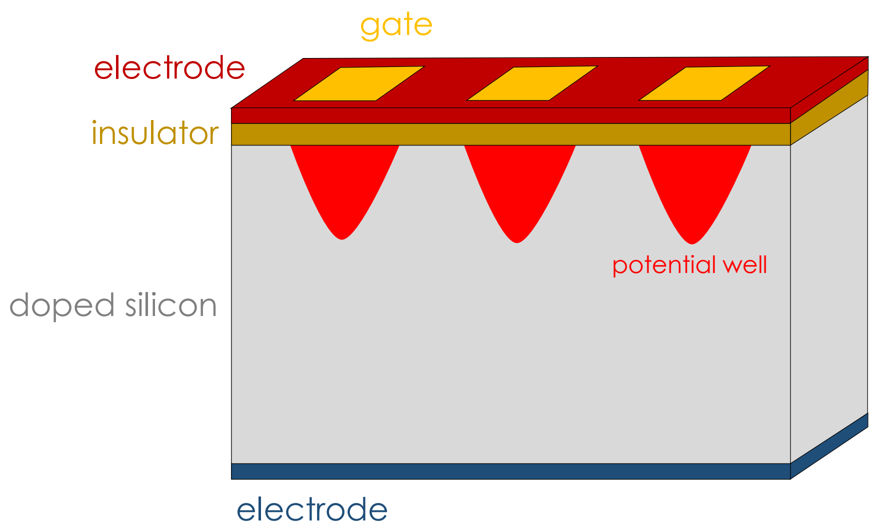


→ interaction creates electron-hole pair

→ pair is separated by voltage

→ One type of charge carrier gets drained by lower electrode

→ remaining charge carriers are collected at insulator and creates charge packages

The created charge packets can then be read-out.

# DAMIC-M

- Abbreviation: DArk Matter In CCDs at Modane
- Successor to DAMIC at SNOLAB, Canada
- DM Direct detection using silicon CCDs with Skipper-CCD
- Achieves single electron resolution → few eV energy resolution

Skipper-CCD:

Method to repeatedly measure the same charge packet in a CCD to reduce noise

the Spokesperson for DAMIC-M is Paolo Privitera from U Chicago

[Papadopoulos for DAMIC-M collab., 2022, https://doi.org/10.1016/j.nima.2022.167184]

# DAMIC-M

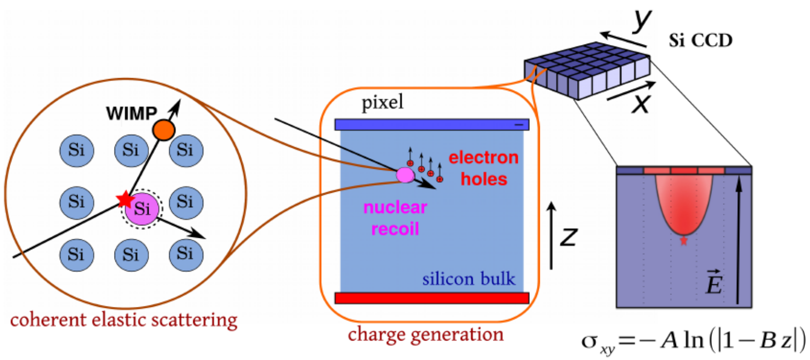


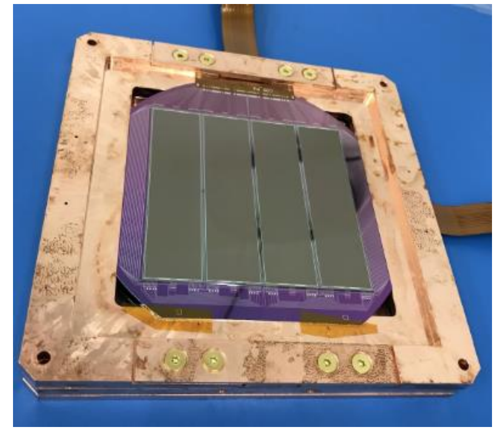

CCD

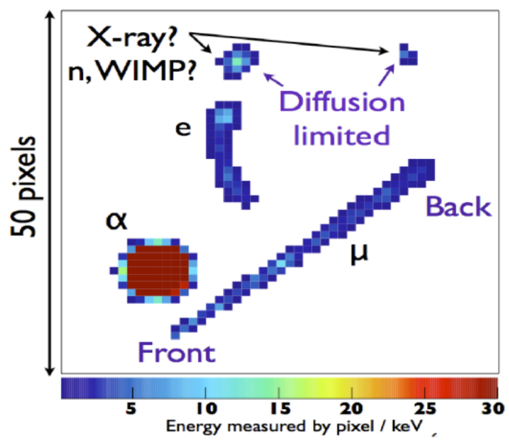


detection process

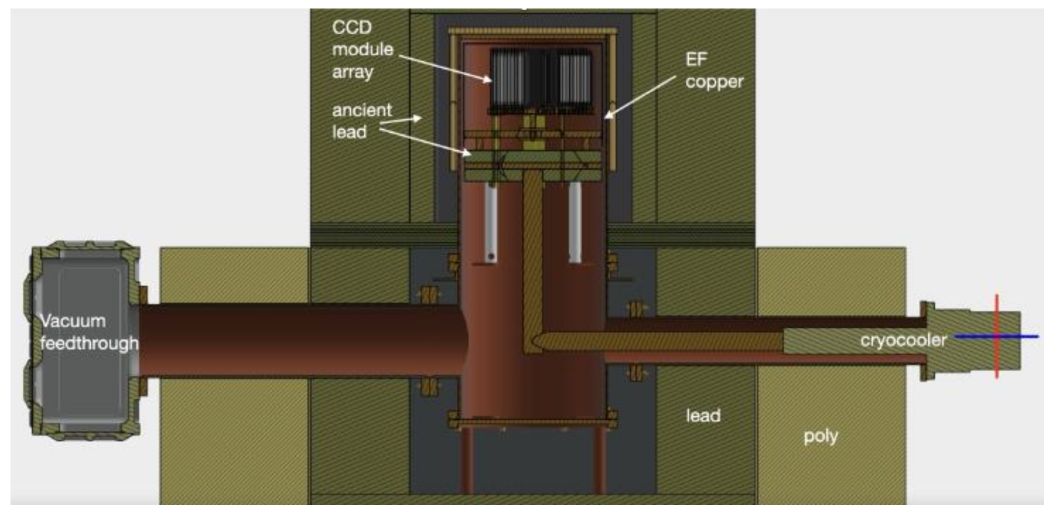


scheduled for 2025

detector set-up

[Privitera for DAMIC-M collab., 2024, https://doi.org/10.22323/1.441.0066 ]

[Castell´o-Mor for DAMIC-M collab., 2022, arXiv:2001.01476]

# UNDERGROUND PRODUCTION

- Our goal is to produce relativistic DM $\chi$ and detect it
- Electron beam in the ~100 MeV range hitting beam dump
- We will be investigating DM-masses of ~1 keV – 1 MeV

rough sketch of set-up

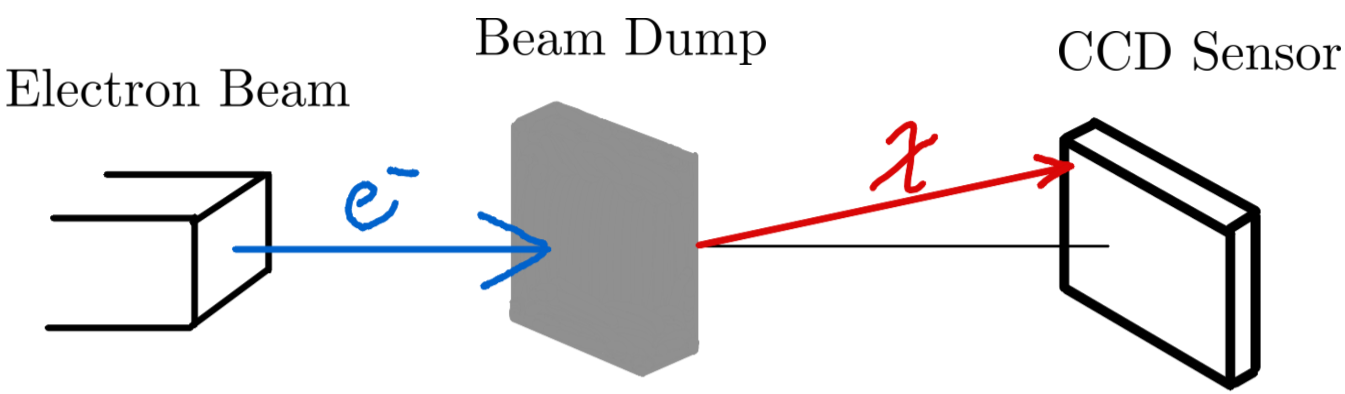

# EM Form Factor Interaction

- We want a model that interacts with the electrons in CCDs
- So we consider: EM form factors & millicharge
- Introduce dark state as a Dirac fermion $\chi$ → From now on, DM will refer to this fermion
  - Millicharge scenario: QED-like interaction term
  - EM form factors: Wilson coefficients of an EFT
- Only requirements on $\chi$ :
  - EFT is valid at the energy of the experiment
  - Not allowed to probe potential inner structure at our energy

based on: Chu, Pradler and Semmelrock, 2018, arXiv:1811.04095

# EM Form Factor Interaction

## Lagrangians and Feynman-Rules:

millicharge ($\varepsilon e$): $\mathcal{L}_{\varepsilon e} = \varepsilon e\, \bar{\chi}\gamma^\mu \chi A_\mu$

magnetic dipole moment - MDM ($\mu_\chi$): $\mathcal{L}_{MDM} = \frac{1}{2}\mu_\chi\, \bar{\chi}\sigma^{\mu\nu}\chi F_{\mu\nu}$

electric dipole moment - EDM ($d_\chi$): $\mathcal{L}_{EDM} = \frac{i}{2} d_\chi\, \bar{\chi}\sigma^{\mu\nu}\gamma^5 \chi F_{\mu\nu}$

anapole moment - AM ($a_\chi$): $\mathcal{L}_{AM} = -a_\chi\, \bar{\chi}\gamma^\mu\gamma^5\chi\partial^\nu F_{\mu\nu}$

charge radius - CR ($b_\chi$): $\mathcal{L}_{CR} = b_\chi\, \bar{\chi}\gamma^\mu\chi\partial^\nu F_{\mu\nu}$

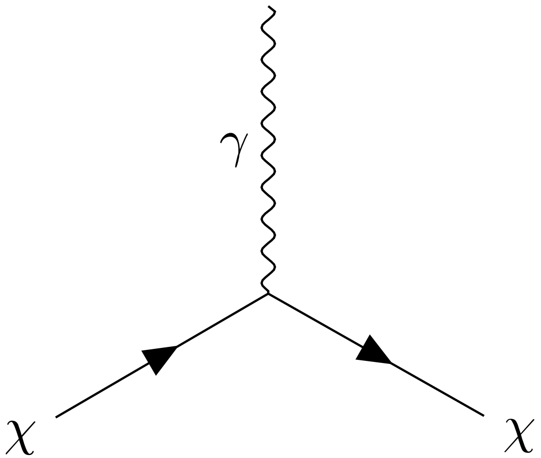


$$\begin{aligned}
\varepsilon e:\quad & i\Gamma^\mu_\varepsilon(q) = i\varepsilon e\gamma^\mu \\
\text{MDM:}\quad & i\Gamma^\mu_M(q) = -\mu_\chi\sigma^{\mu\nu}q_\nu \\
\text{EDM:}\quad & i\Gamma^\mu_E(q) = -id_\chi\sigma^{\mu\nu}\gamma^5 q_\nu \\
\text{AM:}\quad & i\Gamma^\mu_A(q) = -ia_\chi(q^2\gamma^\mu - q^\mu \not{q})\gamma^5 \\
\text{CR:}\quad & i\Gamma^\mu_C(q) = ib_\chi(q^2\gamma^\mu - q^\mu \not{q})
\end{aligned}$$

# UV-Complete Example: Millicharge

Millicharged DM arises in massless Dark Photon theories:

Introduce two U(1) gauge fields $\hat{A}_\mu$ and $\bar{A}_\mu$.

These couple to the SM current $J_\mu$ and the dark current $J'_\mu$. → Includes our $\chi$

The interaction Lagrangian with the kinetic mixing $\varepsilon$ is:

$$\mathcal{L} = -\frac{\varepsilon}{2}\hat{F}^{\mu\nu}\bar{F}_{\mu\nu} + \hat{g}J'^{\mu}\hat{A}_\mu + \bar{g}J^{\mu}\bar{A}_\mu$$

Introduce $A_\mu$ and $A'_\mu$ by diagonalising the kinetic term:

$$\mathcal{L}' = \hat{g}J'^{\mu}A'_\mu + \left(-\frac{\hat{g}\varepsilon}{\sqrt{1-\varepsilon^2}}J'^{\mu} + \frac{\bar{g}}{\sqrt{1-\varepsilon^2}}J^{\mu}\right)A_\mu$$

$A_\mu$ is the usual photon field and $A'_\mu$ is the dark photon field.

Redefine charges to get the electric charge $e$ and the dark charge $e'$:

$$\mathcal{L}' = -e'\sqrt{1-\varepsilon^2}J'^{\mu}A'_\mu + (\varepsilon e' J'^{\mu} + eJ^{\mu})A_\mu$$

Photon now couples to the dark current with a millicharge

[Fabbrichesi et al., 2020, arXiv:2005.01515]

# UV-Complete Examples: MDM

EM form factors can arise from loop effects in a UV-complete theory:

Consider a massive scalar $S$ charged under $\mathrm{U}_Y(1)$ with hypercharge $Y = 1$.

Introduce a Yukawa interaction of a singlet Dirac fermion $\chi$ with leptons $\psi_l$

$$\mathcal{L}_S = -y_l S \bar{\chi} P_R \psi_l + \text{h.c.}, \quad y_l \text{...Yukawa coupling}$$

Take the following diagram and match it to the MDM effective operator:

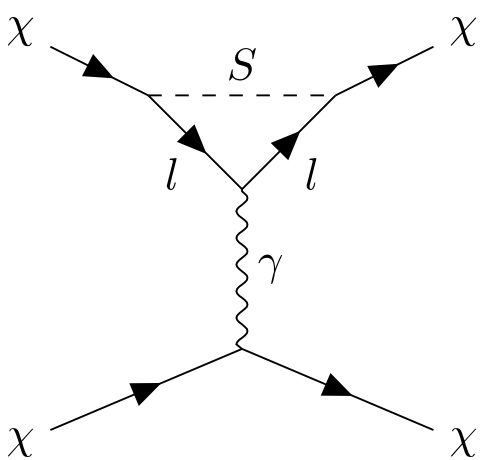


Electric charge of lepton

Lepton mass

$$\approx -\mu_\chi \sigma^{\mu\nu} q_\nu \quad \Rightarrow \mu_\chi \sim \frac{y_l^2 Q}{M} \frac{m_l}{M}$$

Mass of scalar

[Kavanagh et al., 2018, arXiv:1810.00033]

# KINEMATIC SET-UP

- Production by 2→4 electron-electron bremsstrahlung
  - 4-body phase space, determined by beam energy $E_2$
  - Wanted variables: DM energy, DM angle $E_\chi, \cos\theta_\chi$
- Detection through 2→2 DM-electron scattering:
  - 2-body phase space, determined by incoming DM energy $E_\chi$
  - Wanted variable: electron recoil energy $E_R$

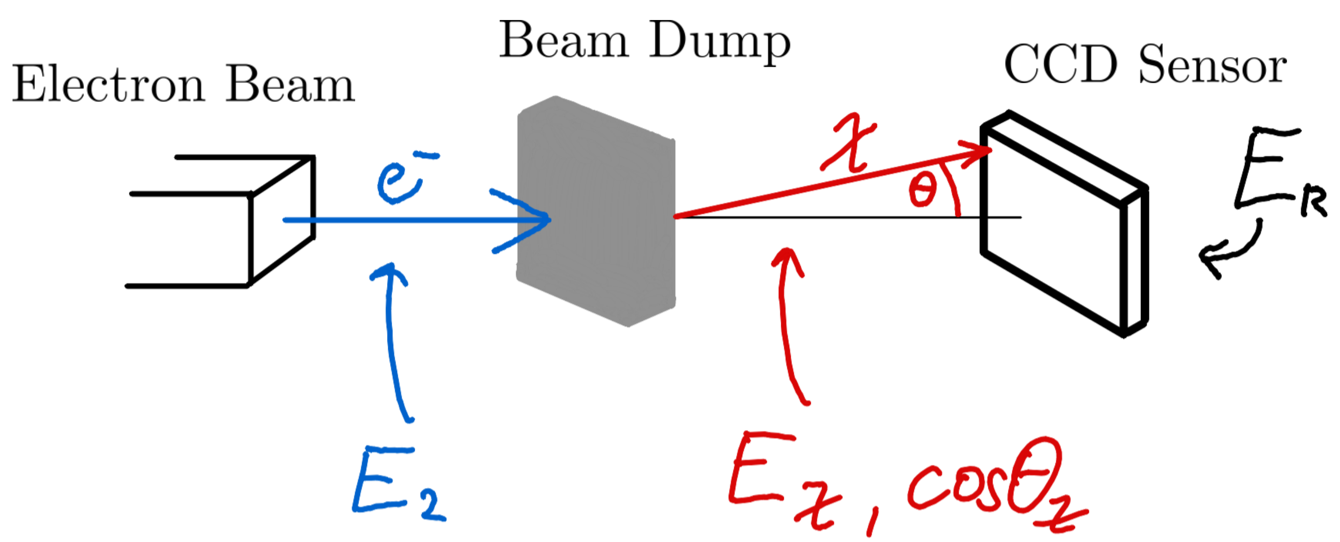

# BREMSSTRAHLUNG PAIR-PRODUCTION

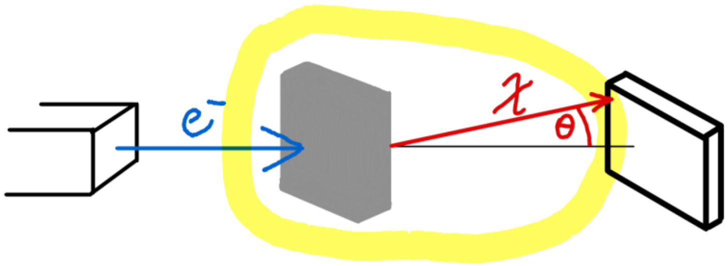


We want to compute the pair-production cross section by 2→4 scattering in the rest frame of the beam dump:

$$\frac{d\sigma_{\text{prod}}}{dE_\chi d\cos\theta_\chi} = \frac{|\vec{p}_\chi|}{4m_e|\vec{p}_2|}\int \frac{d\Pi_{2\to4}}{ds_{34\bar{\chi}}dt_{2\chi}}\frac{1}{|J|}\left|\overline{\mathcal{M}}_{2\to4}\right|^2$$

Related to a variable transformation

$\left|\overline{\mathcal{M}}_{2\to4}\right|^2$ is the spin-summed squared matrix element for bremsstrahlung-like pair-production

Importantly, we focus only on electron-electron scattering as for comparatively low beam energy ~100 MeV, nuclear interactions are kinematically supressed by $\left(\frac{m_e}{m_N}\right)^2$

# Pair-Production Diagrams

We calculate for each form factor separately at tree-level

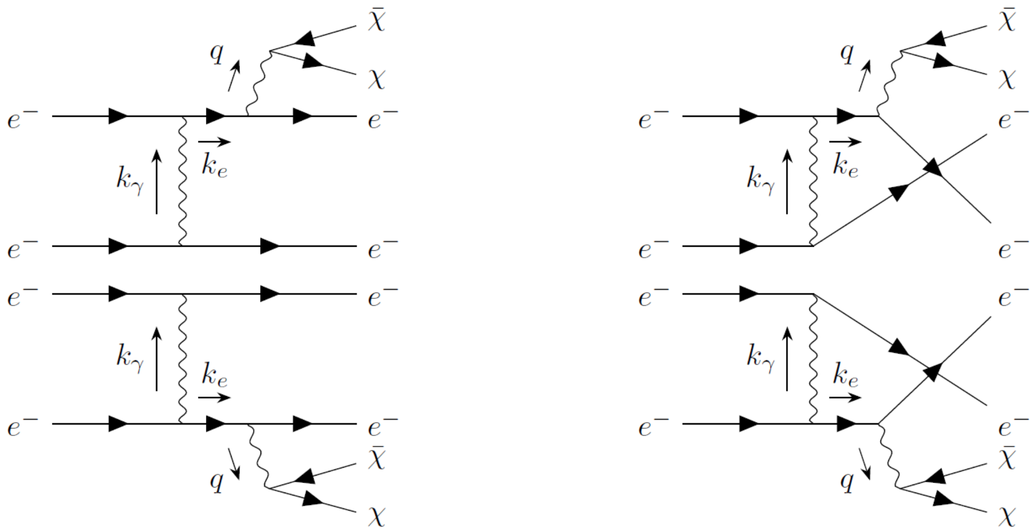


Final state radiation (FSR)

Initial state radiation (ISR)

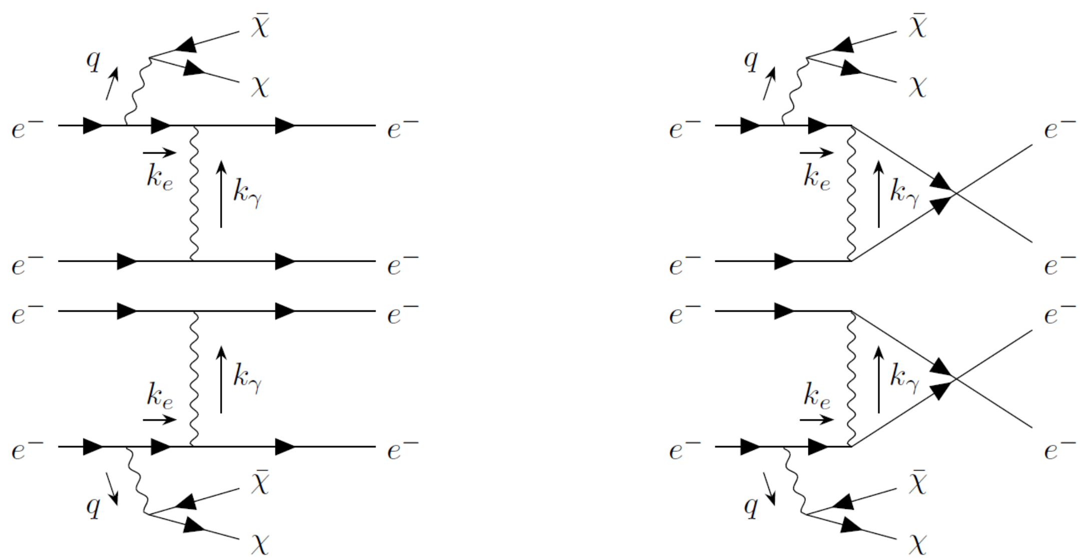

# Phase Space Integration

- General procedure for larger phase spaces:
  - Count relativistic degrees of freedom
  - Pick appropriate Lorentz invariants for the problem
  - Decompose full phase space into 2-body subspaces
  - Integrate subspaces in suitable reference frames
  - Combine results and express the integrated phase space in terms of invariants
  - Choose a frame and variables to do the final cross section computation in

[Byckling & Kajantie: Particle Kinematics, 1973]

# Production: 4-body Phase Space

In order to perform the phase space integration, we need to know its degrees of freedom.

This will be the dimension of the integral.

- For $2 \rightarrow n$ scattering, we get 3 DOF in our phase space from each outgoing 4-momentum from the on-shell condition
- DOF reduced by 4 due to energy-momentum conservation
- Further reduction from rotational redundancy in spin-independent scattering

$$\mathrm{DOF} = 3n - 5$$

So in our case, for n=4, we have 7 independent Lorentz invariants.

The goal is to evaluate the phase space analytically!

# Production: 4-body Phase Space

We have the pair-production process

$$e^-(p_1) + e^-(p_2) \to e^-(p_3) + e^-(p_4) + \chi(p_\chi) + \bar{\chi}(p_{\bar{\chi}})$$

Our input parameters are
$\{p_1 \cdot p_2, m_e, m_\chi\}$

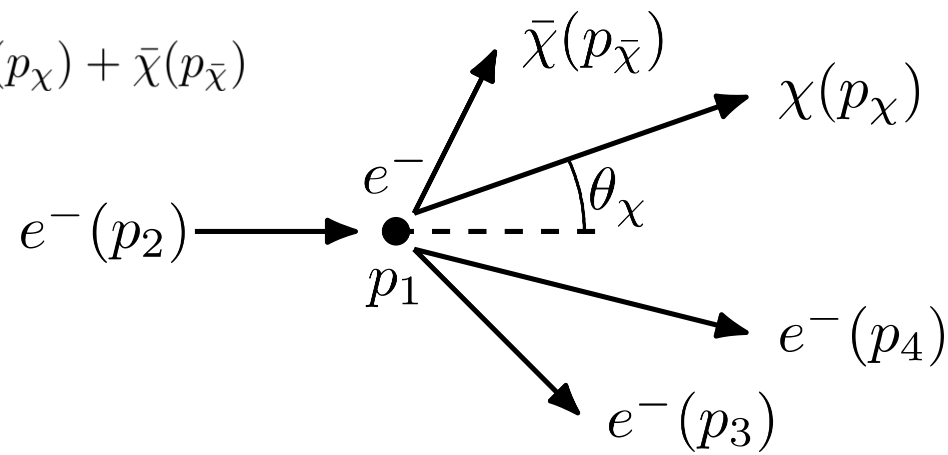


Good choice of Lorentz invariants for our problem:

$$s_{4\bar{\chi}} = (p_4 + p_{\bar{\chi}})^2,\ s_{34\bar{\chi}} = (p_3 + p_4 + p_{\bar{\chi}})^2,\ t_{14} = (p_1 - p_4)^2$$
$$t_{13} = (p_1 - p_3)^2,\ t_{2\chi} = (p_2 - p_\chi)^2,\ p_2 \cdot p_3,\ p_3 \cdot p_4$$

This set is useful for our result being dependent on the DM angle and energy, we focus on χ, not on its antiparticle and integrate:

$$d\Pi_4(p_3, p_4, p_\chi, p_{\bar{\chi}}) = \prod_i \frac{d^3 p_i}{(2\pi)^3 2E_{p_i}} (2\pi)^4 \delta^4\left(p_1 + p_2 - \sum_i p_i\right)$$

# 4-BODY PHASE SPACE: 1ST SUBSPACE

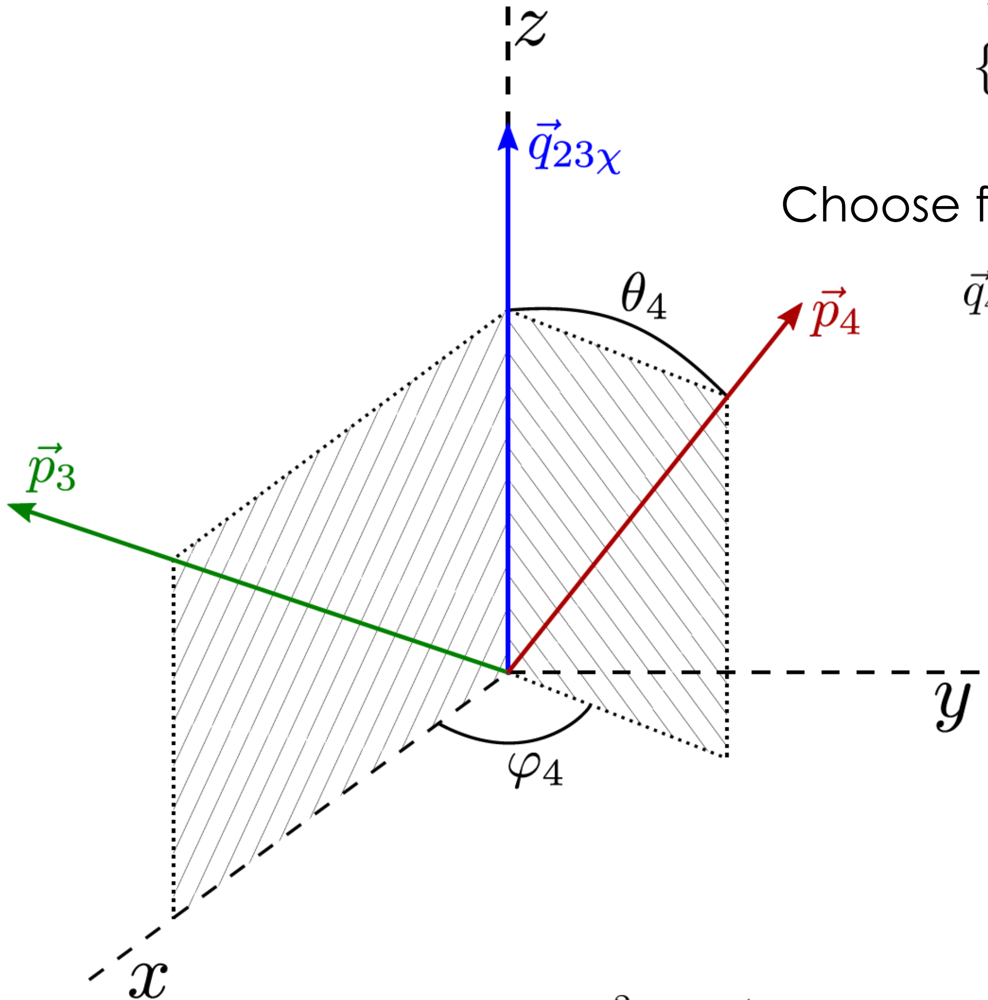


The first system consists of

$$\{q_{4\bar{\chi}} = p_4 + p_{\bar{\chi}}, q_{23\chi}, p_3, p_4\}$$

Choose frame

$$\vec{q}_{4\bar{\chi}} = 0,\ \vec{q}_{23\chi} \parallel z\text{-axis},\ \ \vec{p}_3 \parallel xz\text{-plane}$$

Where: $q_{23\chi}^2 = (p_2 - p_3 - p_\chi)^2 = 2m_e^2 + s_{4\bar{\chi}} + t_{2\chi} - s_{34\bar{\chi}} - t_{13}$

# 4-body Phase Space: 1st Subspace

- We insert $1 = \int \frac{ds_{4\bar{\chi}}}{2\pi} \frac{d^3 q_{4\bar{\chi}}}{(2\pi)^3 2E_{4\bar{\chi}}} (2\pi)^4 \delta^{(4)}(q_{4\bar{\chi}} - p_4 - p_{\bar{\chi}})$ into the full integral

  and reduce the integration over $p_4, p_{\bar{\chi}}$

- We then get

$$\int \frac{d^3 p_4}{(2\pi)^3 2E_4} \frac{d^3 p_{\bar{\chi}}}{(2\pi)^3 2E_{\bar{\chi}}} (2\pi)^4 \delta^{(4)}(q_{4\bar{\chi}} - p_4 - p_{\bar{\chi}}) = \int \frac{d\cos\theta_4}{2\pi} \frac{d\varphi_4}{2\pi} \frac{P_4}{4\sqrt{s_{4\bar{\chi}}}}$$

- Here the azimuthal angle $\varphi_4$ expresses the Lorentz invariant $p_3 \cdot p_4$

- Finally, we transform the polar angle into $dt_{14} = -2P_4 \sqrt{\vec{q}^{\,2}_{23\chi}}\, d\cos\theta_4$

- The integrated subsystem is thus

$\lambda(a, b, c) = (a - b - c)^2 - 4bc$

$$d\Phi(q_{4\bar{\chi}}) = -\int \frac{dt_{14}}{2\pi} \frac{d\varphi_4}{2\pi} \frac{1}{4} \lambda^{-1/2}(s_{4\bar{\chi}}, m_e^2, q_{23\chi}^2)$$

# 4-body Phase Space: 2$^{\text{ND}}$ Subspace

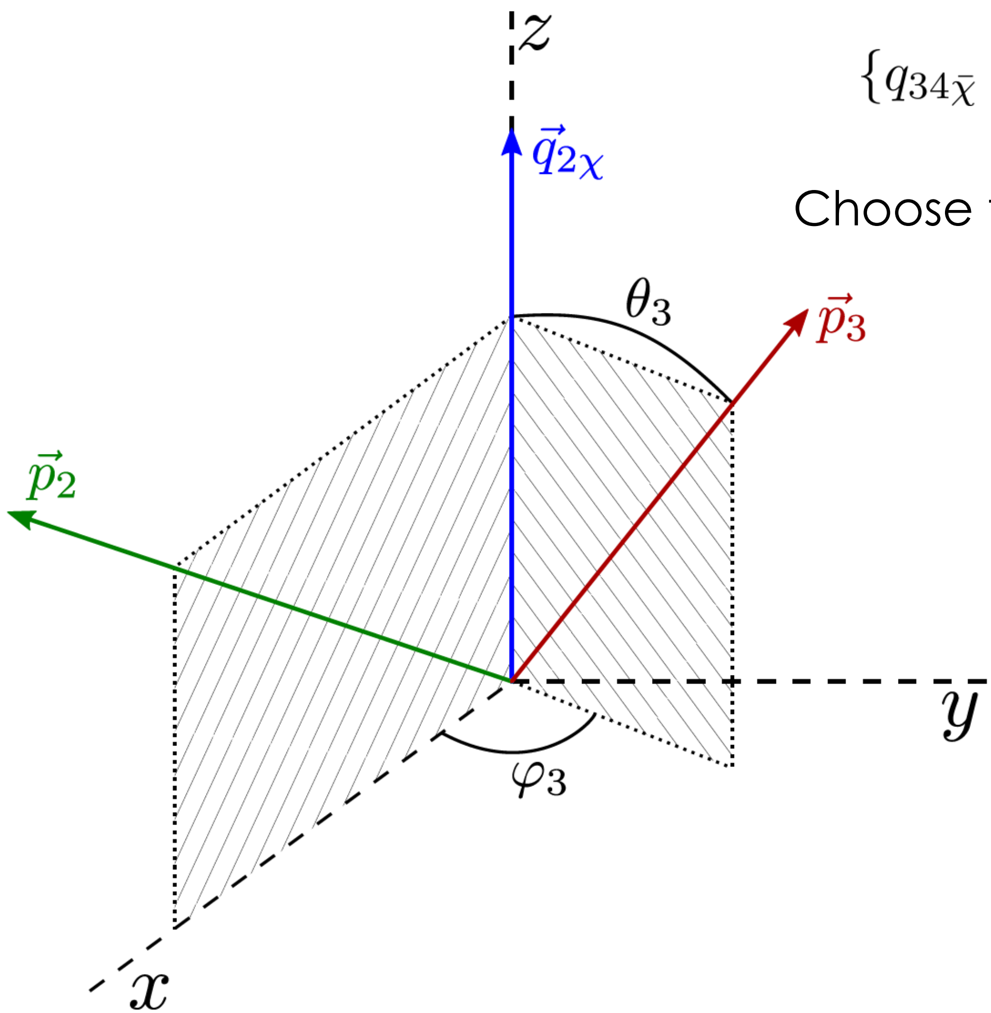


The first system consists of

$$\{q_{34\bar{\chi}} = p_3 + p_4 + p_{\bar{\chi}}, q_{2\chi} = p_2 - p_\chi, p_2, p_3\}$$

Choose frame

$$\vec{q}_{34\bar{\chi}} = 0,\ \vec{q}_{2\chi} \parallel z\text{-axis},\ \ \vec{p}_2 \parallel xz\text{-plane}$$

# 4-BODY PHASE SPACE: 2ND SUBSPACE

- We insert $1 = \int \frac{ds_{34\bar{\chi}}}{2\pi} \frac{d^3 q_{34\bar{\chi}}}{(2\pi)^3 2E_{34\bar{\chi}}} (2\pi)^4 \delta^{(4)}(q_{34\bar{\chi}} - p_3 - q_{4\bar{\chi}})$ into the full integral

  and reduce the integration over $p_3, q_{4\bar{\chi}}$

- We then get

$$\int \frac{d^3 q_{4\bar{\chi}}}{(2\pi)^3 2E_{4\bar{\chi}}} \frac{d^3 p_3}{(2\pi)^3 2E_3} (2\pi)^4 \delta^{(4)}(q_{34\bar{\chi}} - q_{4\bar{\chi}} - p_3) = \int \frac{d\cos\theta_3}{2\pi} \frac{d\varphi_3}{2\pi} \frac{P_3}{4\sqrt{s_{34\bar{\chi}}}}$$

- Here the azimuthal angle $\varphi_3$ expresses the Lorentz invariant $p_2 \cdot p_3$

- Finally, we transform the polar angle into $dt_{13} = -2P_3\sqrt{\vec{q}_{2\chi}^{\,2}}\, d\cos\theta_3$

- The integrated subsystem is thus

$$d\Phi(q_{34\bar{\chi}}) = -\int \frac{dt_{13}}{2\pi} \frac{d\varphi_3}{2\pi} \frac{1}{4} \lambda^{-1/2}(s_{34\bar{\chi}}, m_e^2, t_{2\chi})$$

# 4-BODY PHASE SPACE: LAB SYSTEM

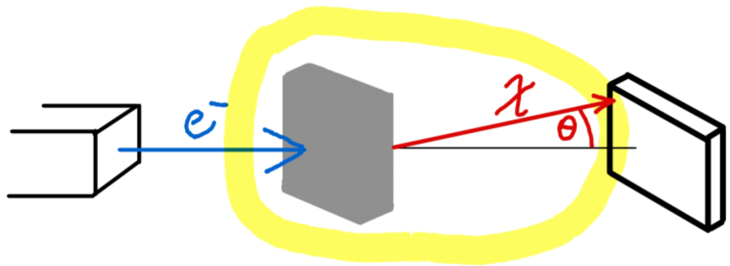


- We want to reduce out the remaining momentum integrals
- We do the remaining integration in the LAB frame of the beam dump, which also corresponds to the physical set-up of the problem: $p_1 = (m_e, \vec{0}),\ \vec{p}_2 \parallel z\text{-axis}$
- We insert $1 = \int \frac{d^3 q_{2\chi}}{2E_{2\chi}} dt_{2\chi} \delta^{(3)}(\vec{q}_{2\chi} - \vec{p}_2 + \vec{p}_\chi)\delta(E_{2\chi} - E_2 + E_\chi)$
- Putting the previous results together and integrating out $p_\chi, q_{34\bar{\chi}}$:

$$\boxed{\frac{d\Pi_{2\to 4}}{ds_{34\bar{\chi}}dt_{2\chi}} = \int ds_{4\bar{\chi}} dt_{13} dt_{14} \frac{d\varphi_3}{2\pi}\frac{d\varphi_4}{2\pi}\frac{|J|}{(4\pi)^5}\lambda^{-1/2}(s_{4\bar{\chi}}, m_e^2, q_{23\chi}^2)\lambda^{-1/2}(s_{34\bar{\chi}}, m_e^2, t_{2\chi})}$$

The $|J|$ is related to the variable transform: $\frac{dE_\chi d\cos\theta_\chi}{ds_{34\bar{\chi}}dt_{2\chi}} = \frac{|J|}{|\vec{p}_\chi|} = \frac{1}{4|\vec{p}_2||\vec{p}_\chi|m_e}$

# 4-body Phase Space: Physical Region

- Physical integration limits of Lorentz invariants are obtained through kinematical considerations
- When integrating matrix elements, we need to express all 15 unique scalar products of the system in terms of Lorentz invariants and input parameters
  - One SP given by input energy
  - Seven SP given by Lorentz invariants
  - Six SP given by 4-momentum conservation
- The remaining SP can be expressed using linear dependence

# 4-BODY PHASE SPACE: PHYSICAL REGION

We get the last scalar product using the fact that six vectors in 4D must be linearly dependent.

$p_\chi \cdot p_{\bar{\chi}}$ still has a degeneracy as can be seen from the diagram.

We pick one solution for each half circle of the azimuthal plane $\varphi_4$

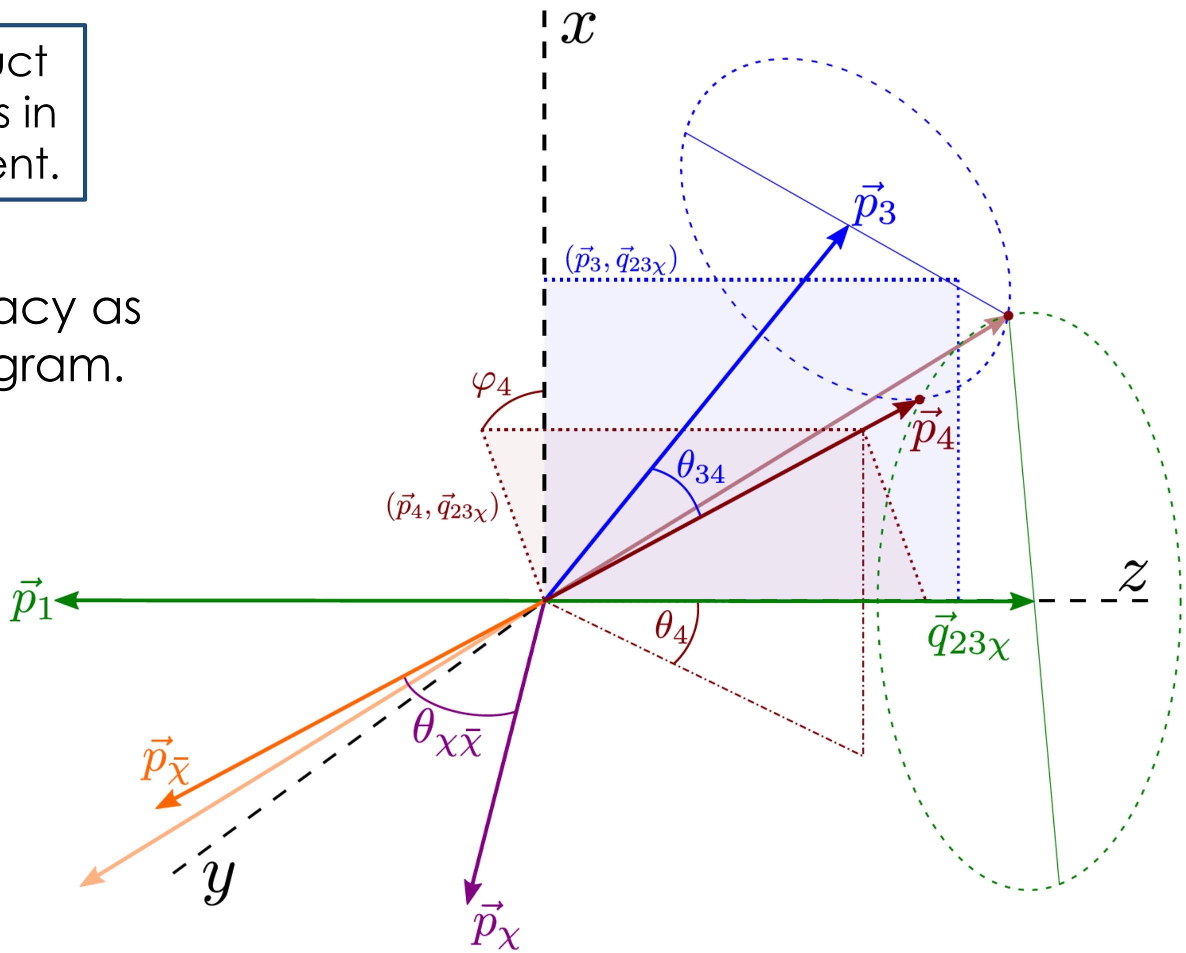


We solve the equation from the determinant of the Gram matrix $\det \mathbf{M} = \det(p_i \cdot p_j) = 0$

# Computational Methods

The matrix elements were calculated symbolically using **Mathemtica** with **FeynCalc**

↓

- To compute the production cross section numerically, we need the 5-dimensional 4-body phase space integration
- Due to the complexity of this integral, we use multidimensional Monte-Carlo integration
- The MC method we use is the **CUBA** library and the calculation implemented using **Fortran**

↓

Further numerics and data analysis is done in **Python**

# Pair-Production Results

Preliminary Results

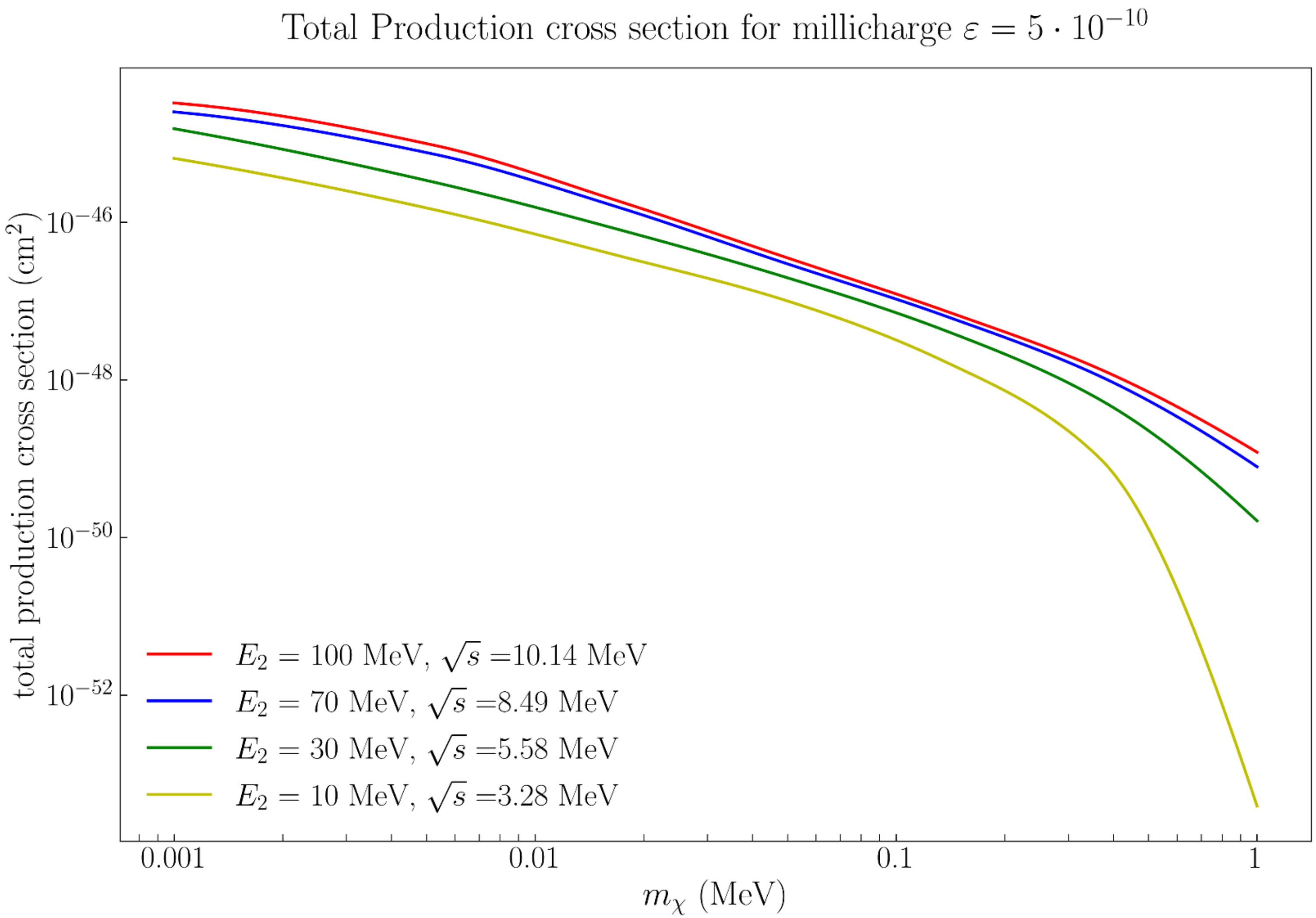

# Detection: 2-body Phase Space

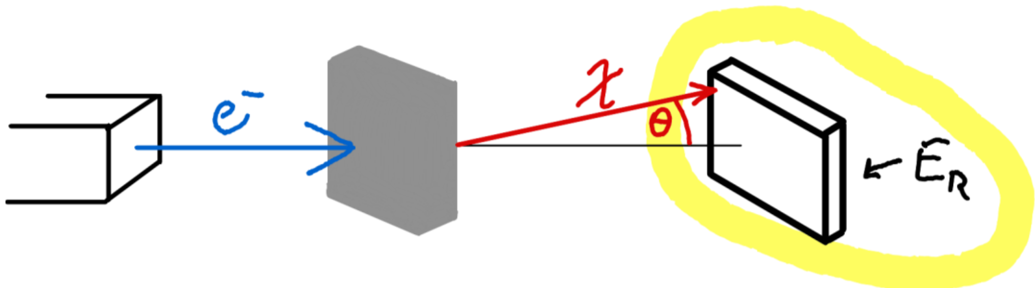


- We again focus on DM-electron scattering
- So we have the detection process in the LAB frame

$$\chi(p_1) + e^-(p_2) \to \chi(p_3) + e^-(p_4)$$

Input parameters: $\{E_\chi, m_e, m_\chi\}$

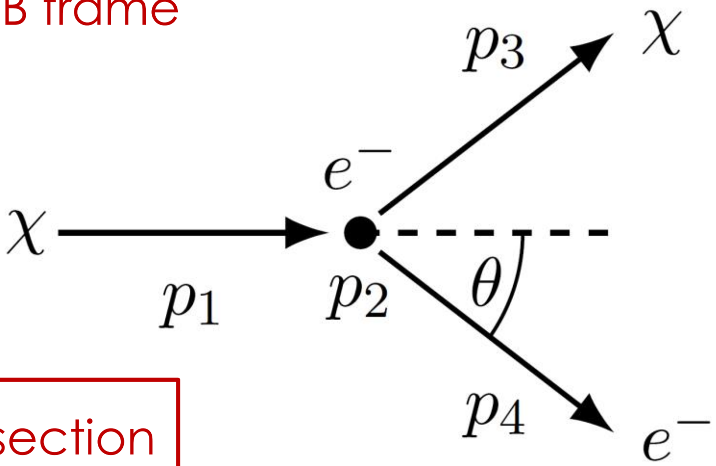


We are interested in the electron recoil cross section with $E_R = E_4 - m_e$ in the LAB frame:

$$\frac{d\sigma}{dE_R} = \frac{|\mathcal{M}|^2}{32\pi m_e (E_\chi^2 - m_\chi^2)}$$

$$p_1 = (E_\chi, \vec{p}_1)$$
$$p_2 = (m_e, \vec{0})$$

# Detection Cross Section

- The resulting detection cross sections at tree level are:

$$\left(\frac{d\sigma}{dE_R}\right)^{\rm det}_{\varepsilon e} = \frac{\pi\varepsilon^2\alpha^2}{m_e^2(E_\chi^2-m_\chi^2)E_R^2}\Big(2m_eE_\chi^2 + m_eE_R(E_R-m_e-2E_\chi) - m_\chi^2E_R\Big)$$

$$\left(\frac{d\sigma}{dE_R}\right)^{\rm det}_{\rm MDM} = \frac{\alpha\mu_\chi^2}{2m_e(E_\chi^2-m_\chi^2)E_R}\Big(2m_e(E_\chi^2 - E_\chi E_R - m_\chi^2) + m_\chi^2E_R\Big)$$

$$\left(\frac{d\sigma}{dE_R}\right)^{\rm det}_{\rm EDM} = \frac{\alpha d_\chi^2}{2m_e(E_\chi^2-m_\chi^2)E_R}\Big(2m_eE_\chi^2 - 2m_eE_\chi E_R - m_\chi^2E_R\Big)$$

$$\left(\frac{d\sigma}{dE_R}\right)^{\rm det}_{\rm AM} = \frac{\alpha a_\chi^2}{(E_\chi^2-m_\chi^2)}\Big(m_e(2E_\chi^2 - 2E_\chi E_R + E_R^2 - 2m_\chi^2) + (m_\chi^2 - m_e^2)E_R\Big)$$

$$\left(\frac{d\sigma}{dE_R}\right)^{\rm det}_{\rm CR} = \frac{\alpha b_\chi^2}{(E_\chi^2-m_\chi^2)}\Big(m_e(2E_\chi^2 - 2E_\chi E_R + E_R^2) - (m_e^2 + m_\chi^2)E_R\Big)$$

- With a maximum recoil energy of

$$E_R^{\rm max} = \frac{2m_e(E_\chi^2-m_\chi^2)}{m_e(2E_\chi+m_e)+m_\chi^2}$$

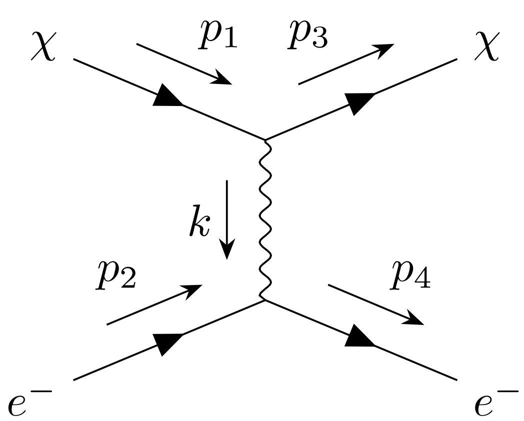

# Detection Event Rate

- The differential event rate at the detector depends on the DM flux of produced particles on it

differential detection cross section

$$\frac{dR_{\rm det}}{dE_R dE_\chi d\cos\theta_\chi} = \frac{dN_{\rm det}}{dt dE_R dE_\chi d\cos\theta_\chi} = N_{\rm det} \frac{d\Phi_\chi}{dE_\chi d\cos\theta_\chi} \frac{d\sigma_{\rm det}}{dE_R}$$

detector target number

- The DM flux at the beam dump in turn depends on the electron beam flux on the target

radiation length of beam dump

$$\frac{d\Phi_\chi}{dE_\chi d\cos\theta_\chi} = X_0 \frac{dN_\chi}{dt dV dE_\chi d\cos\theta_\chi} = X_0 n_T \Phi_e \frac{d\sigma_{\rm prod}}{dE_\chi d\cos\theta_\chi}$$

beam dump number density

- The final differential event rate per recoil energy is therefore

$$\boxed{\frac{dR_{\rm det}}{dE_R} = X_0 n_T N_{\rm det} \Phi_e \int dE_\chi d\cos\theta_\chi \frac{d\sigma_{\rm prod}}{dE_\chi d\cos\theta_\chi} \frac{d\sigma_{\rm det}}{dE_R}}$$

# Detection Event Rate Results

Preliminary Results $X_0 = 0.5$ cm, $n_T = 10^{23}$ cm$^{-3}$, $N_{\rm det} = 7.6 \times 10^{15}$, $\Phi_e = 10^{10}$ cm$^{-2}$ s$^{-1}$

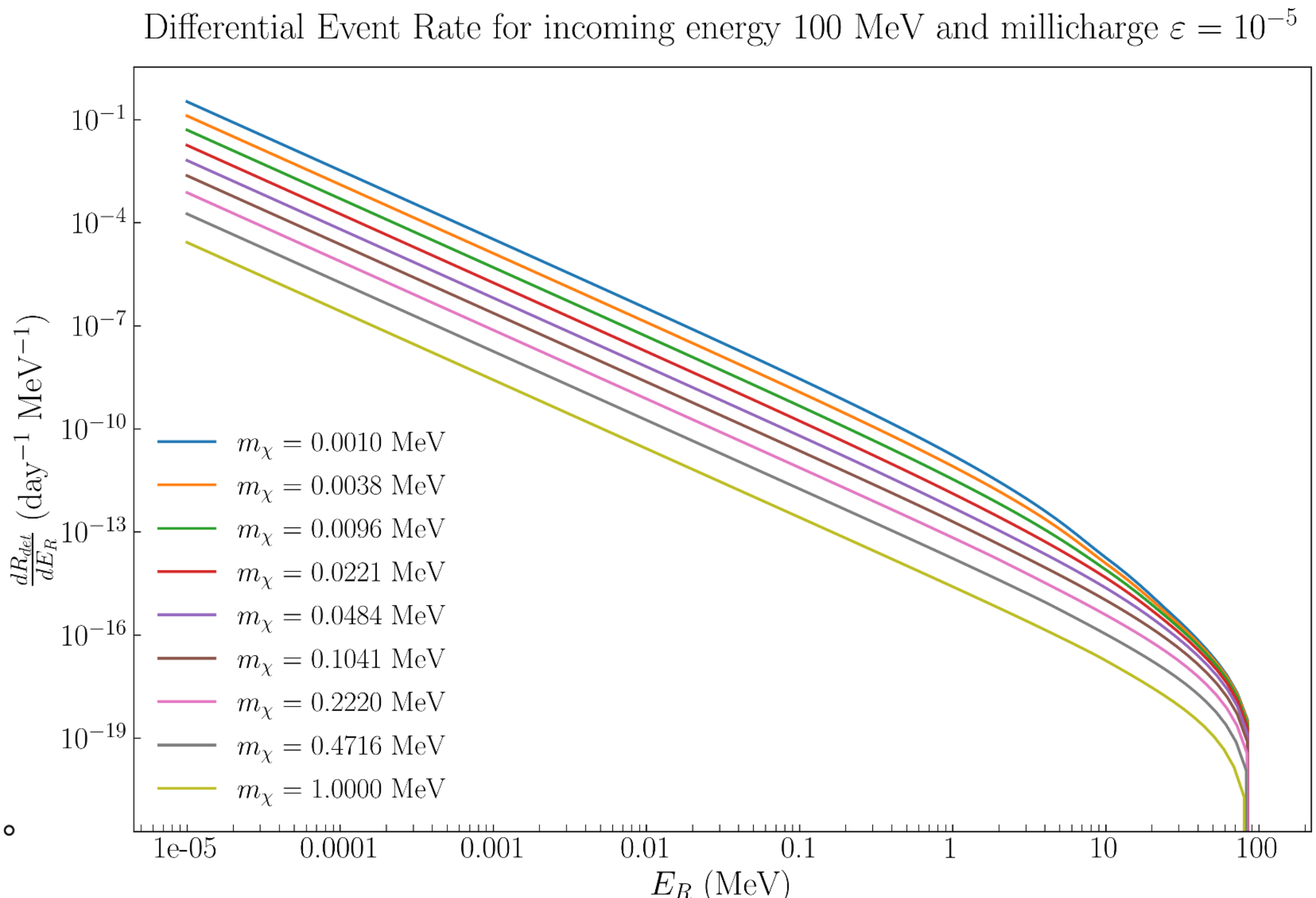


$\theta_\chi^{\rm max} = 30°$

$\sqrt{s} \approx 10$ MeV

# Detection Event Rate Results

Preliminary Results $X_0 = 0.5\ \text{cm},\ n_T = 10^{23}\ \text{cm}^{-3},\ N_{\text{det}} = 7.6 \times 10^{15},\ \Phi_e = 10^{10}\ \text{cm}^{-2}\ \text{s}^{-1}$

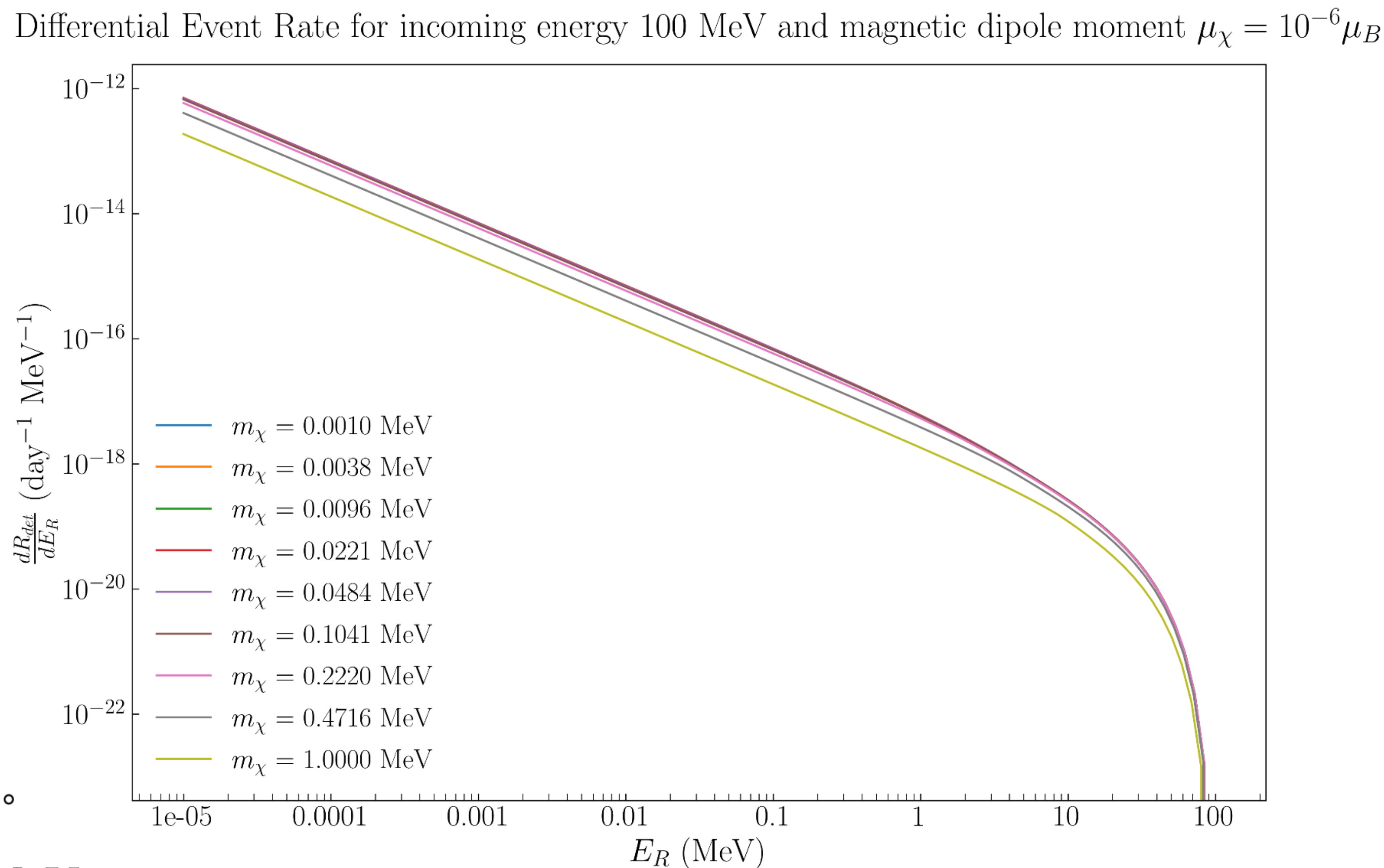


$\theta_\chi^{\max} = 30°$

$\sqrt{s} \approx 10$ MeV

# Detection Event Rate Results

Preliminary Results $X_0 = 0.5$ cm, $n_T = 10^{23}$ cm$^{-3}$, $N_{\text{det}} = 7.6 \times 10^{15}$, $\Phi_e = 10^{10}$ cm$^{-2}$ s$^{-1}$

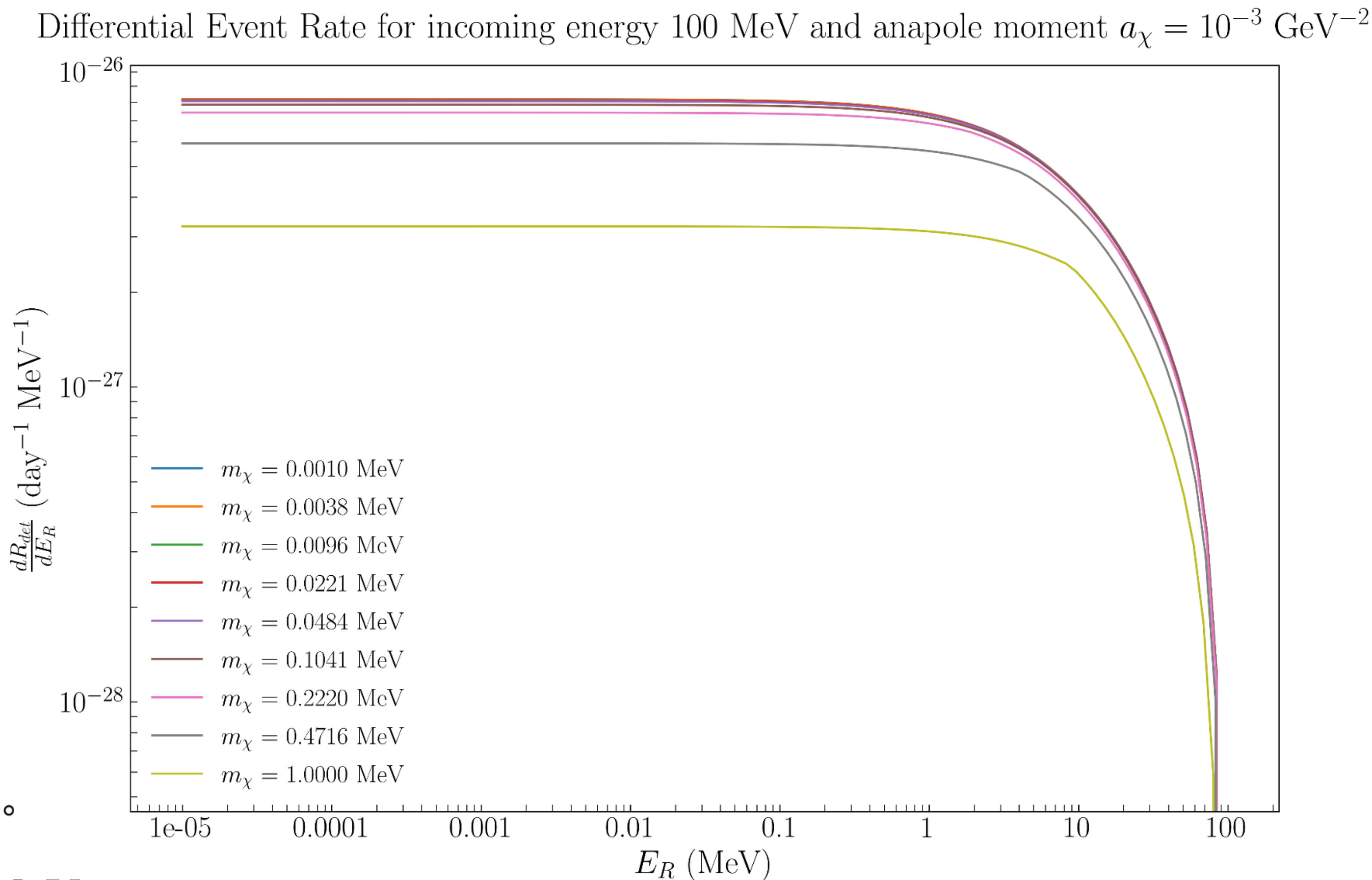


$\theta_\chi^{\max} = 30°$

$\sqrt{s} \approx 10$ MeV

# Corrections To Detection

- Because of sensitivity of the detector, we need to consider low energy corrections to the detection cross section
- Possible bound state corrections are approximately $\frac{d\sigma_1 - d\sigma_0}{d\sigma_0} = 10^{-3}$ which is negligible in our case
- The solid state effects inside the CCD effects can come from phonons and plasmons
- The corrections due to phonons would be of the order of phonon energies of ~0.1-100meV, additionally suppressed by the DM being relativistic and light
- Corrections from plasmon interactions may become important due the plasmon energies of ~1eV → next step

[Plestid, Wise, 2024, arXiv:2403.12184]

# Bounds From High Precision Physics

- We can put bounds on the couplings/mass via measurements from SM precision observables:
  - Running of the fine structure constant

    $$|\mu_\chi|, |d_\chi| < 3.2 \times 10^{-6} \mu_B \qquad |a_\chi|, |b_\chi| < 3.2 \times 10^{-5} \mathrm{GeV}^{-2}$$

  - From anomalous magnetic moments
  - Electron electric dipole moment
  - Missing transverse energy at colliders

    $$|\mu_\chi|, |d_\chi| < 1.3 \times 10^{-5} \mu_B \qquad |a_\chi|, |b_\chi| < 1.5 \times 10^{-5} \mathrm{GeV}^{-2}$$

  - If the particle couples effectively to hypercharge, the invisible Z-width

[Chu, Pradler, Semmelrock, 2018, arXiv:1811.04095]

# Bounds From Astrophysics

- If our new fermion is dark matter, then we get constraints from cosmology and astrophysics:
  - Direct detection of local dark matter abundance
  - Dark matter kinetic decoupling and dampening of LSS
  - Self-scattering effect in DM halos
  - Supernova cooling due to additional channel
  - DM annihilation in CMB and galactic centres

[Chu, Pradler, Semmelrock, 2018, arXiv:1811.04095]

# Bounds

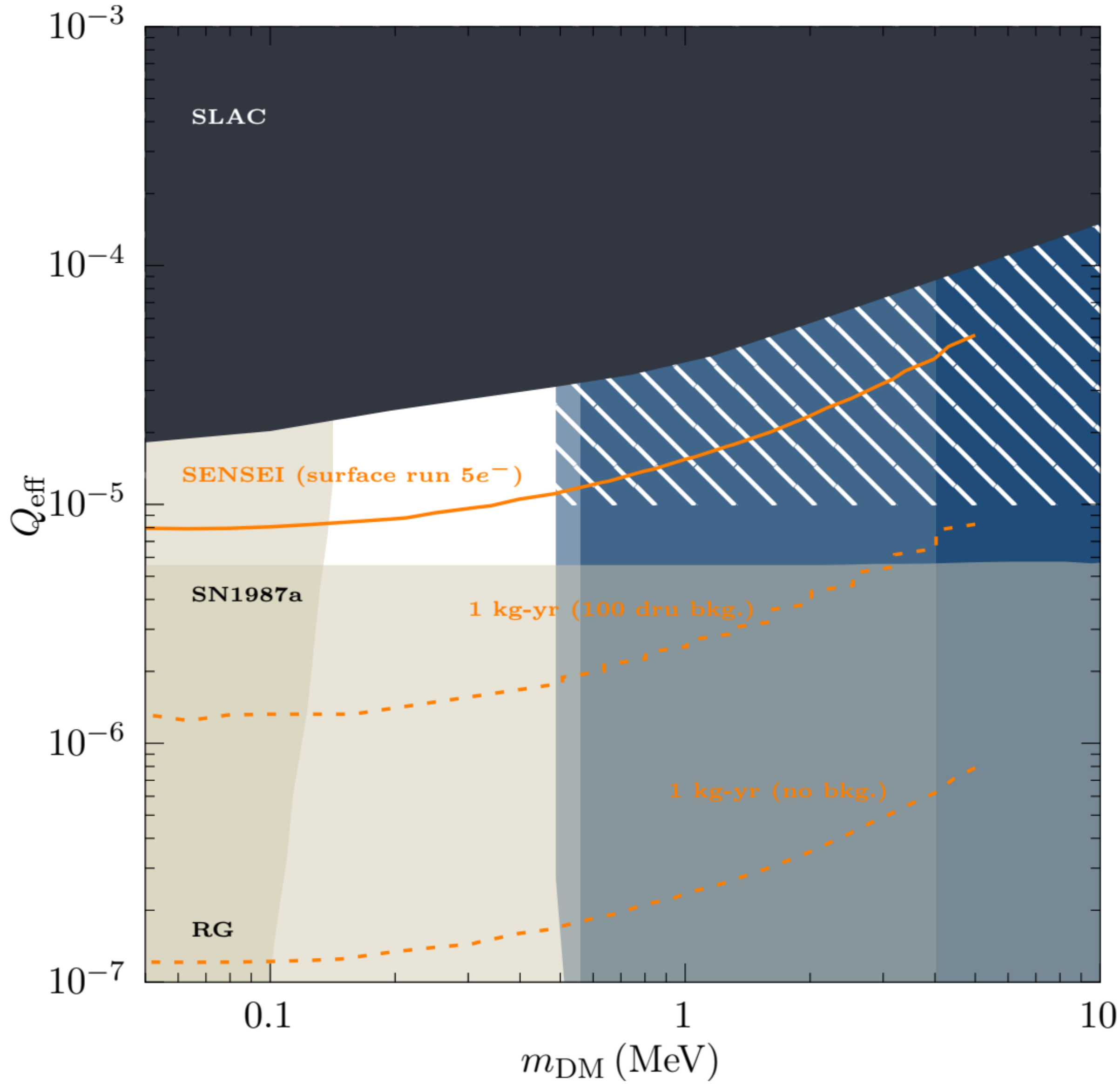


[An et al., 2021, arXiv:2108.10332]

# BOUNDS

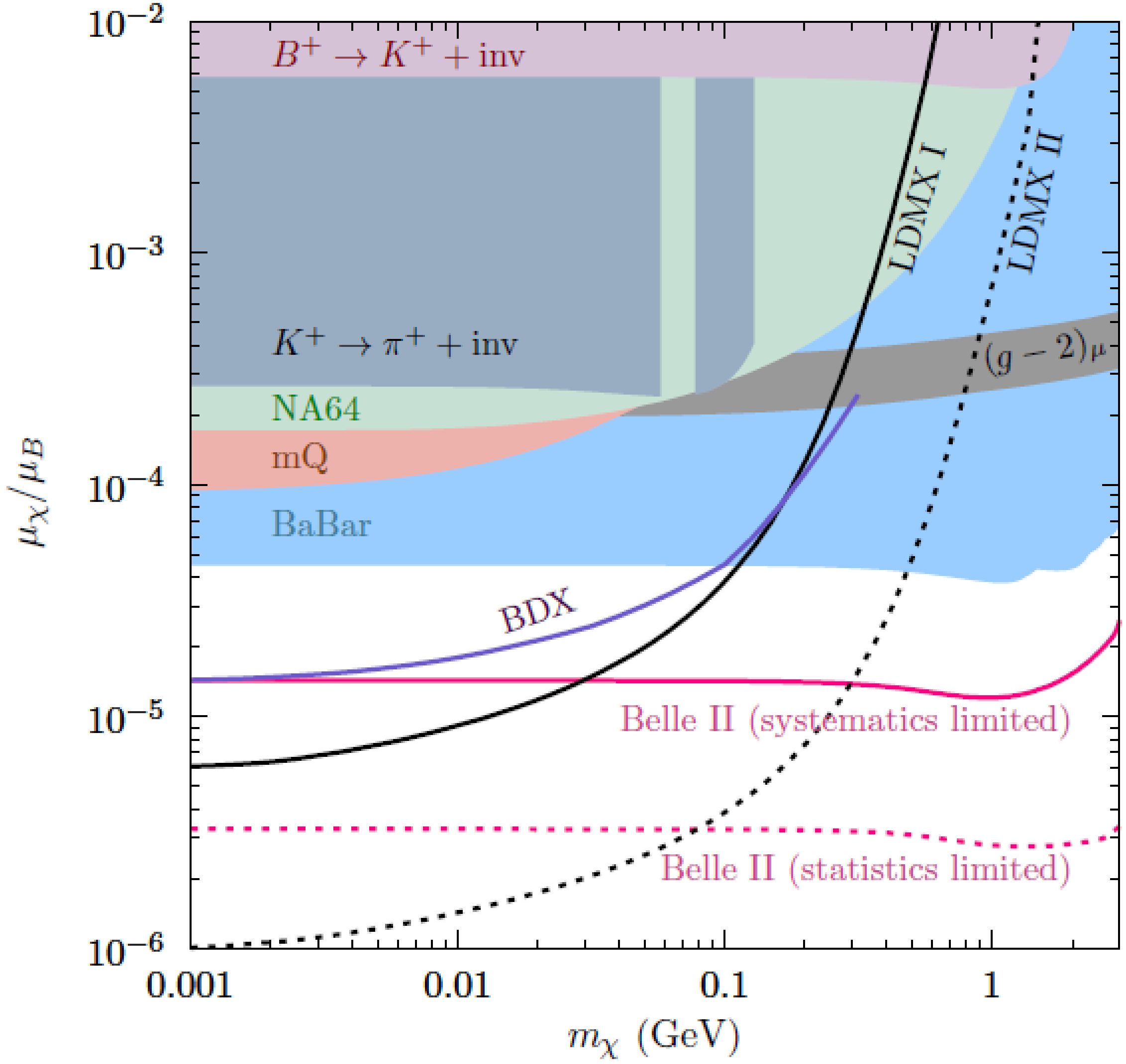


[Chu, Pradler, Semmelrock, 2018, arXiv:1811.04095]

# Bounds

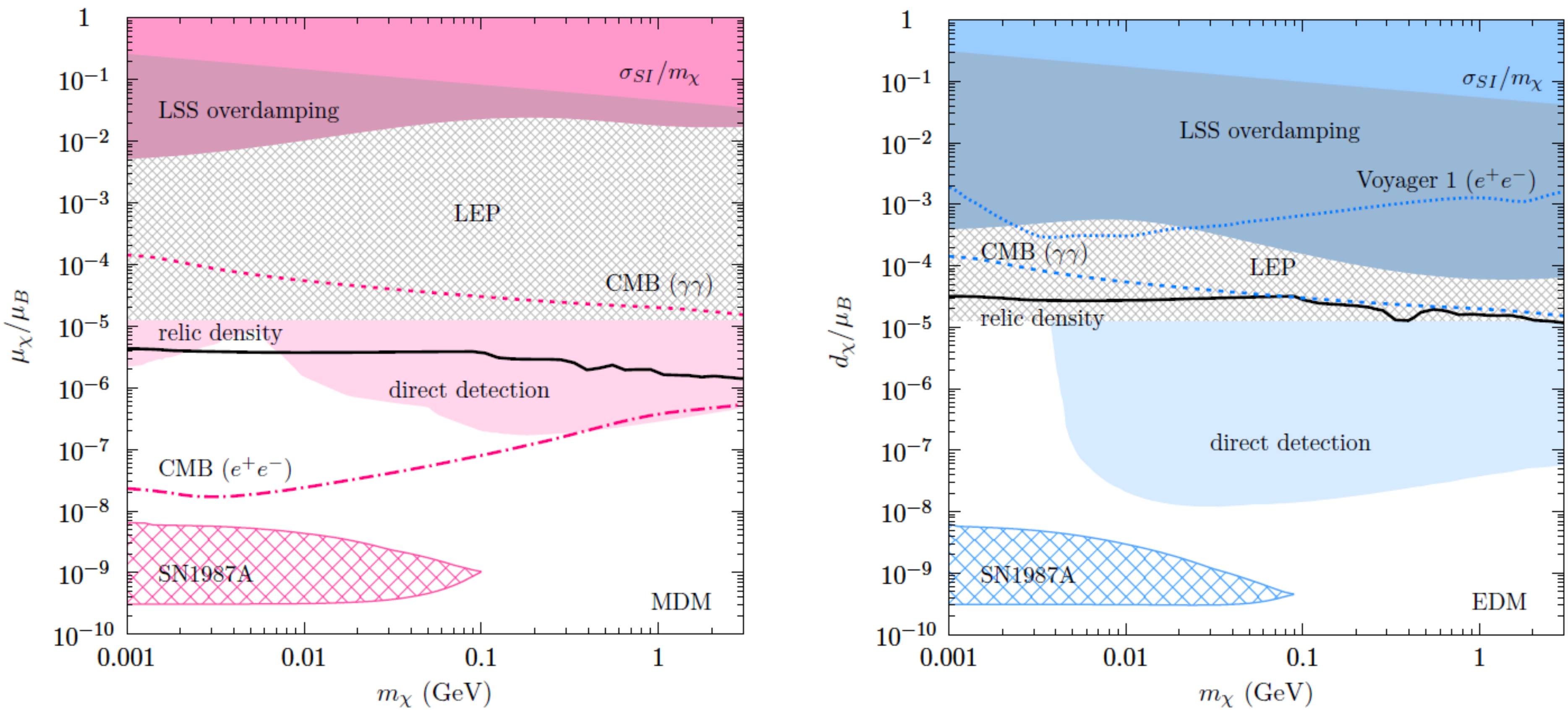


[Chu, Pradler, Semmelrock, 2018, arXiv:1811.04095]

# Closing Remarks

- Things to still to be done:
  - Get concrete experimental set-up from the DAMIC-M team
  - Calculate plasmon corrections to the detection cross section
  - Derive bounds for the mass ranges discussed

# Thank you!

Special thanks to the Faculty of Physics and the Vienna Doctoral School of Physics for their generous support as a recipient of a Master Fellowship!

# Additional Slides

# Higher Order Couplings

- Additionally, we can consider 7-dimensional operators, called (pseudo)-Rayleigh or susceptibility operators:

scalar Rayleigh interaction - SR ($r_\chi$): $$\mathcal{L}_{Rs} = \frac{1}{4} r_\chi \, \bar{\chi}\chi F_{\mu\nu} F^{\mu\nu}$$

pseudoscalar Rayleigh interaction - PR ($\tilde{r}_\chi$): $$\mathcal{L}_{Rp} = \frac{i}{4} \tilde{r}_\chi \, \bar{\chi}\gamma^5 \chi F_{\mu\nu} \tilde{F}^{\mu\nu}$$

- These give rise to the Feynman rules:

$$\text{SR:} \quad i\Gamma^{\mu\nu}_{Rs}(q_1, q_2) = i r_\chi (q_2^\mu q_1^\nu - q_1 \cdot q_2 \eta^{\mu\nu}),$$

$$\text{PR:} \quad i\Gamma^{\mu\nu}_{Rp}(q_1, q_2) = -\tilde{r}_\chi \gamma^5 \varepsilon^{\mu\nu\sigma\rho} q_{1\sigma} q_{2\rho}.$$

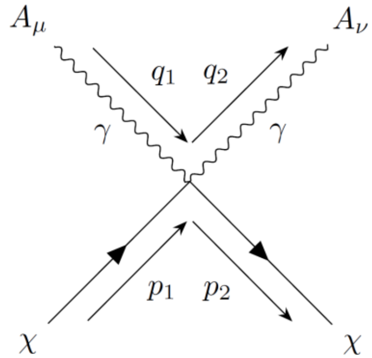


- But as higher dimensional coupling are even more supressed as well as these vertices only contributing to our processes starting at one loop, we can safely neglect them

# Non-Relativistic Correspondence

- The EM form factors receive their names due their non-relativistic correspondence to QM operators
- This can be seen by expanding the matrix element with an external EM field in the limit p/m→0
- This corresponds to the Born approximation with some potential, that can be identified with a NR interaction
- As an example, the MDM operator coupled to an external vector potential:

$$\frac{1}{2m_\chi}\Big(i\mu_\chi \bar{u}^s(p_2)\sigma^{\mu\nu}q_\nu u^r(p_1)\Big)A^{\mathrm{ex}}_\mu \xrightarrow{NR} \frac{1}{2m_\chi}\Big(i\mu_\chi(-2m_\chi\xi_s^\dagger(-i\varepsilon^{jil}q^i\sigma^l)\xi_r\Big)A^j(\vec{q})$$
$$= \xi_s^\dagger\Big(i\mu_\chi\varepsilon^{ijl}q^iA^j(\vec{q})\sigma^l)\Big)\xi_r \xrightarrow{FT} \xi_s^\dagger\Big(-\mu_\chi\varepsilon^{ijl}\partial^iA^j(\vec{x})\sigma^l)\Big)\xi_r = \xi_s^\dagger\Big(-\mu_\chi B^l(\vec{x})\sigma^l)\Big)\xi_r$$

# Relativistic Angle Relation

- For the angles in the two sub phase spaces we have

$$p_2 \cdot p_3 = \frac{(p_1 \cdot p_2) G(p_1, p_1 - p_\chi; p_1 - p_\chi, p_3)}{-\Delta_2(p_1, p_1 - p_\chi)} - \frac{((p_1 - p_\chi) \cdot p_2) G(p_1, p_1 - p_\chi; p_1, p_3)}{-\Delta_2(p_1, p_1 - p_\chi)} - \frac{\sqrt{\Delta_3(p_1, p_1 - p_\chi, p_2) \Delta_3(p_1, p_1 - p_\chi, p_3)}}{-\Delta_2(p_1, p_1 - p_\chi)} \cos\varphi_3 .$$

$$p_3 \cdot p_4 = \frac{(p_1 \cdot p_3) G(p_1, q_{23\chi}; q_{23\chi}, p_4)}{-\Delta_2(p_1, q_{23\chi})} - \frac{(q_{23\chi} \cdot p_3) G(p_1, q_{23\chi}; p_1, p_4)}{-\Delta_2(p_1, q_{23\chi})} - \frac{\sqrt{\Delta_3(p_1, q_{23\chi}, p_3) \Delta_3(p_1, q_{23\chi}, p_4)}}{-\Delta_2(p_1, q_{23\chi})} \cos\varphi_4$$

$$\Delta_n(p_1, \ldots, p_n) = \det\left((p_1, \ldots, p_n)^T (p_1, \ldots, p_n)\right)$$

$$G(p_1, \ldots, p_n; q_1, \ldots, q_n) = \det\left((p_1, \ldots, p_n)^T (q_1, \ldots, q_n)\right)$$

[Byckling & Kajantie: Particle Kinematics, 1973]

# 4-BODY PHASE SPACE: PHYSICAL REGION

- Physical integration limits of Lorentz invariants: $\varphi_3 \in [0, 2\pi), \ \varphi_4 \in [0, 2\pi)$

$$(2m_e + m_\chi)^2 \leq s_{34\bar{\chi}} \leq (\sqrt{s} - m_\chi)^2$$

$$(m_e + m_\chi)^2 \leq s_{4\bar{\chi}} \leq (\sqrt{s_{34\bar{\chi}}} - m_e)^2$$

$$\begin{aligned}[t_{2\chi}]^\pm = m_e^2 + m_\chi^2 - \frac{1}{2}(s + m_\chi^2 - s_{34\bar{\chi}}) \\ \pm \frac{1}{2s}\lambda^{1/2}(s, m_e^2, m_e^2)\lambda^{1/2}(s, s_{34\bar{\chi}}, m_\chi^2)\end{aligned}$$

$$\begin{aligned}[t_{14}]^\pm = 2m_e^2 - \frac{1}{2s_{4\bar{\chi}}}(s_{4\bar{\chi}} + m_e^2 - q_{23\chi})(s_{4\bar{\chi}} + m_e^2 - m_\chi^2) \\ \pm \frac{1}{2s_{4\bar{\chi}}}\lambda^{1/2}(s_{4\bar{\chi}}, q_{23\chi}, m_e^2)\lambda^{1/2}(s_{4\bar{\chi}}, m_\chi^2, m_e^2)\end{aligned}$$

$$\begin{aligned}[t_{13}]^\pm = 2m_2^2 - \frac{1}{2s_{34\bar{\chi}}}(s_{34\bar{\chi}} + m_e^2 - t_{2\chi})(s_{34\bar{\chi}} + m_e^2 - s_{4\bar{\chi}}) \\ \pm \frac{1}{2s_{34\bar{\chi}}}\lambda^{1/2}(s_{34\bar{\chi}}, t_{2\chi}, m_e^2)\lambda^{1/2}(s_{34\bar{\chi}}, s_{4\bar{\chi}}, m_e^2)\end{aligned}$$

# 4-BODY PHASE SPACE: LAB VARIABLES

- While a Lorentz invariant phase space is very general, it is more convent to work with variables tailored to the problem
- In our case, we want to use the energy and angle of the produced particles, so we transform

$$E_\chi = \frac{1}{2}m_e + E_2 - \frac{1}{2m_e}(s_{34\bar{\chi}} - t_{2\chi}), \ \cos\theta_\chi = \frac{s_{34\bar{\chi}} - 2me^2 - m_\chi^2 + 2E_2E_\chi + 2m_eE_\chi - 2m_eE_2}{2\sqrt{E_\chi^2 - m_\chi^2}\sqrt{E_2^2 - m_e^2}}$$

- We get the limits:

$$E_\chi \geq \frac{m_\chi(2m_e + E_2)}{\sqrt{2me(m_e + E_2)}}$$

$$E_\chi \leq \frac{E_2}{2} + \frac{2m_e + E_2}{2m_e(m_e + E_2)}\left(m_\chi^2 - (2m_e + m_\chi)^2\right) + \frac{\sqrt{E_2^2 - m_e^2}}{4m_e(m_e + E_2)}\sqrt{2m_eE_2 - 3m_e^2}\sqrt{2m_eE_2 - 2(m_e^2 + 2m_\chi^2 + 4m_em_\chi)}$$

$$1 \leq \cos\theta_\chi \leq \max\left(-1, \frac{E_2(E_\chi - m_e) + m_e(E_\chi + 2m_\chi + m_e)}{\sqrt{E_\chi^2 - m_\chi^2}\sqrt{E_2^2 - m_e^2}}\right)$$

Angle accounts for relativistic boosting